Int J Adv Manuf Technol (2015) 77:1549–1555
DOI 10.1007/s00170-014-6517-9

ORIGINAL ARTICLE

Experimental evaluation of polycrystalline diamond (PCD) tool geometries at high feed rate in milling of titanium alloy TC11

Wei Ji · Xianli Liu · Lihui Wang · Shilong Sun

Received: 2 July 2014 / Accepted: 17 October 2014 / Published online: 14 November 2014

Abstract Titanium alloys are widely used in aerospace industrial components characterised by high material removal rate, of which the machining efficiency is a big issue. Targeting the problem, this paper presents the experimental findings of milling of titanium alloy TC11 using polycrystalline diamond (PCD) cutting tool at high feed rate. First, in order to verify the capability of PCD in finish milling of titanium alloys at high feed rate, the surface roughness R_a is investigated under different PCD tool geometries (radial rake angle, axial rake angle and insert sharp radius), and the results indicate that its range is from 0.821 to 1.562 μm, which is suitable to titanium components. Also, the main tool failure patterns, cutting edge fracture and flank face wear, are observed and classified. Based on the tool failure patterns, the relationship between tool life and tool geometries is established. In order to explain the reasons of tool failures, the relationships between cutting forces and the tool geometries are made clear. Finally, the processes of flank face wear and rake face wear of PCD insert are proposed to show its wear evaluations.

Keywords High-feel milling · PCD · Tool geometries · Titanium alloy TC11

W. Ji · X. Liu (✉) · L. Wang · S. Sun
Harbin University of Science and Technology, 150080 Harbin, China
e-mail: xlliu@hrbust.edu.cn

W. Ji
e-mail: weiji@hrbust.edu.cn

L. Wang
e-mail: lihui.wang@iip.kth.se

W. Ji · L. Wang
KTH Royal Institute of Technology, 10044 Stockholm, Sweden

1 Introduction

Titanium alloys are widely used in the aerospace industry due to their good strength-to-weight ratio and superior corrosion resistance [1]. Also, titanium alloy components are characterised by high removal rate, e.g. with five-axis machining of aerospace structural components, where up to 90 % of the raw materials can be removed during machining [2]; therefore, it is important to increase the efficiency for titanium alloys machining. However, titanium alloys are well known as difficult-to-cut materials due to their low thermal conductivity and high strength. Therefore, tool life and machining integrity are the big challenges for increasing machining efficiency [3]. Considering these problems, many research efforts have focuses on tool material selection [4–9], e.g. uncoated vs. coated carbide, polycrystalline cubic boron nitride (PCBN), polycrystalline diamond (PCD), as well as high-efficiency cutting methods [10–13], e.g. high-speed cutting, high performance cooling.

Many research works were reported on the performance comparison between PCD and the other tool materials. A comparison study between PCD and PCBN in turning was carried out by Nabhani [14], the results of which demonstrate that PCD has the lowest wear rate. Similar conclusions were achieved by Su et al. [15]. The test results indicate that the tool life of PCD is much longer than that of PCBN tools under the same cutting conditions and the average surface roughness produced during machining using PCD inserts is lower compared to that using PCBN inserts. Also, a PCD tool exhibits better performance than an uncoated or coated carbide tool. Amin et al. [16] indicated this point from more detailed aspects, e.g. cutting vibrations, cutting parameter ranges, and tool wear rate. Oosthuizen et al. [17] reported that the tool life of a PCD tool was higher than a coated carbide tool in milling of Ti-6Al-4V when the cutting speed is beyond 100 m/min. Also, Corduan et al. [18] studied the wear mechanism of

PCBN, PCD and TiB_2-coated carbide, and their test results of turning of Ti-6Al-4V indicated that a PCD tool has the best performance with v_c=150 m/min.

On the other hand, researchers also focused on the high-efficiency machining method, i.e. high-speed machining. Based on the experiment of PCD cutter milling of Ti-6Al-4V blades, Kuljanic et al. [19] reported that the performance of PCD was high, and both high tool life and low surface roughness could be achieved under 110-m/min cutting speed, 0.135/z feed per tooth, and 0.2-mm axial depth of cut. In [11], Li et al. tested different cutting speeds (250, 375, 500, 625, 750, and 1000 m/min) in milling of Ti-6Al-4V, and the results demonstrated that when cutting speed is more than 375 m/min, the breakage at cutting edge was observed. Moreover, Sutter et al. [20] carried out orthogonal cutting tests in which the range of cutting speed was from 300 to 4400 m/min (5–75 m/s) by using uncoated carbide, to propose a detailed analysis of geometry of the chip alloy Ti–6Al–4V.

In summary, PCD is regarded as the most suitable tool material for machining titanium alloys among the current tool materials. Also, when cutting speed is too high, the tool breakage is the main problem that is difficult to address, i.e. there may be an insurmountable point by increasing cutting speed to increase machining efficiency. Therefore, new methods to increase machining efficiency are needed. More recently, feed rate cutting methods have been promoted by many cutting tool companies to raise rough and semi-finish machining efficiency. However, few studies have been devoted to high feed milling in finish machining, concerning the poor surface roughness generated at high feed cutting using the carbide tools. Considering the high hardness and high tartness of the PCD tool, the authors wondered whether a good surface roughness and an ideal tool wear could be obtained in high feed milling by using a PCD tool. Unfortunately, there are no suitable PCD tools, and most of them are not designed for high feed milling. Targeting the suitable PCD tool geometries for high feed milling, the main objective of this paper is to investigate and establish the effects between tool geometries and tool performance (surface roughness, tool failure patterns, cutting force, and tool wear process, etc.) in milling of titanium alloys at high feed rate.

2 Experimental methodologies

2.1 Workpiece material

The workpiece material used in the machining test is TC11 (35 HRC and 1030 MPa yield strength). The chemical composition of TC11 confirms to be the following specification (in weight percentage): 6.3 % Al, 3.2 % Mo, 1.2 % Zr, 0.26 % Si, 0.202 % Fe, 0.05 % C, 0.03 % N, 0.001 % H, 0.16 % O, and with the balance of titanium.

2.2 Cutting tool

Figure 1a shows the tool holder and the insert used in the test. The tool holder is DMC320H (KYOCERA) with a single insert seat equipped with 0° rake angle at both radial and axial directions. The insert is divided into two parts, carbide body and PCD, where the carbide body is NDCW150308FRX (KYOCERA) and the PCD material is CTB010 (element six) with 10-μm grain size. The two parts are joined together using high-frequency brazing. The insert's geometry parameters are shown in Fig. 1b, e.g. radial rake angle (RRA), axial rake angle (ARA) and insert sharp radius (ISR).

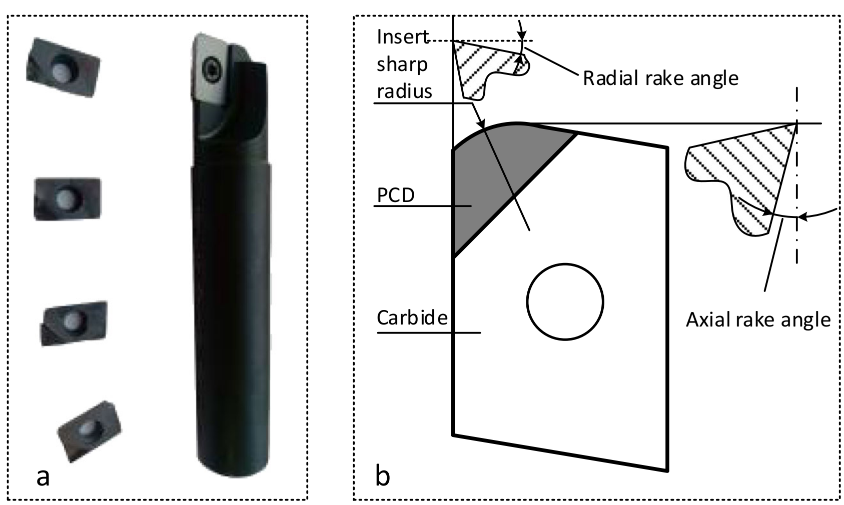

Fig. 1 Test insert geometry parameters. **a** Tool holder and inserts. **b** Geometrical dimensions of tool insert

Table 1 Cutting tool geometry parameters

	Factor		
	Radial rake angle	Axial rake angle	Insert sharp radius
Level 1	6	1	0.8
Level 2	11	5	1.6
Level 3	1	9	2.4

Flank angle of all inserts is 7°

2.3 Other equipment

The face milling test was carried out on a VDL-1000E four-axis machine tool. A high lubricity emulsion (pH 8.5–9) was used at a consistency of 5 %. Conventional cooling was applied overhead at a flow rate of 2.7 L/min. Kistler 9257B multicomponent force plate was used to measure cutting force, and the data acquisition system DH5922 was applied to collect the cutting force data (peak-to-peak). KEYENCE VHX1000 digital microscope was used to observe tool wear.

2.4 Test method

In order to understand the relationship between tool performance and tool geometries, Taguchi method was chosen. Table 1 shows the test data including three factors and three levels. The tests were carried out under a group of cutting parameters (150-m/min cutting speed, 0.5-mm/z feed per tooth, 0.08-mm cutting depth and 15-mm cutting width).

3 Results and discussions

The experimental results are given in Table 2, which include PCD insert geometry parameters, i.e. RRA, ARA and ISR, as well as measured test parameters, e.g. cutting forces (in feed direction F_f, cutting width direction F_e and tool axis direction F_a), surface roughness R_a and machining time t (see tool life definition in 3.2). To obtain all relationship between tool geometry parameters and those objectives, all data were analysed by using range analysis method (see Eqs. 1 and 2) [21], where the values of $\overline{K}_{ij}$ were used to describe those relationship.

$$K_{ij} = \sum_{k=1}^{j} r_{ik} \tag{1}$$

$$\overline{K}_{ij} = \frac{K_{ij}}{j} \tag{2}$$

where r_{ik} represents the measured test result, i is the factor number and j the count of levels. $\overline{K}_{ij}$ represents the influence parameter of factor i.

3.1 Surface roughness

The trend of the calculated surface roughness R_a is depicted in Fig. 2 a–c for RRA, ARA and ISR, respectively. From the figure, the surface roughness is more sensible for RRA, and an increasing trend is observed when RRA increases. ARA and ISR apparently only have minor influence on the roughness. Therefore, RRA plays a key role in surface roughness.

Table 2 Taguchi experimental results

Insert no.	Rake angle		Tool sharp radius (mm)	Cutting force (N)			Roughness R_a (μm)	Machining time t (min)
	Radial (°)	Axial (°)		F_f	F_e	F_a		
1	6	5	0.8	461.4	346.7	363.8	1.118	8.5
2	11	1	0.8	368.7	466.2	378.1	1.364	19.5
3	1	9	0.8	322.3	361.3	80.6	0.980	37
4	6	1	1.6	324.2	363.8	373.5	1.097	24.5
5	11	9	1.6	550.2	830	329.6	1.562	1
6	1	5	1.6	241.6	184.5	68.6	0.821	76.1
7	6	9	2.4	478.5	512.6	351.6	1.120	1
8	11	5	2.4	297.9	336.8	263.7	1.314	1
9	1	1	2.4	166.1	138.6	100.1	0.919	29.5

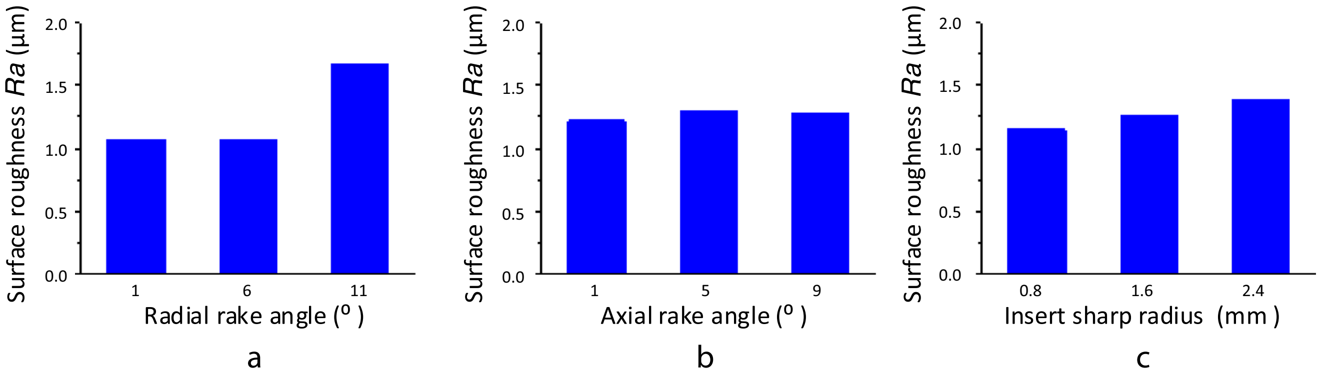

Fig. 2 Surface roughness at varying tool geometries. **a** Radial rake angle. **b** Axial rake angle. **c** Insert sharp radius

Moreover, all of the R_a measurements obtained in machining at high feed are located between 0.821 and 1.562 μm, and they were found to be bigger than those obtained in high-speed machining [16]. For the case with high requirement of surface roughness, high feed machining with PCD tool may not be suitable, e.g. most of pneumatic parts. However, it may be used in machining of those components with low and medium roughness requirements, e.g. some structural parts.

3.2 Tool failure patterns and tool life

PCD tool material possesses low strength and high brittleness, despite high hardness. Due to these properties, tool failure pattern is a critical factor for judging whether PCD tool has the capability to machine titanium alloys at high feed. Therefore, the inserts were examined using optical microscope after set cutting intervals, and the wear was continuously observed. Figure 3 shows the classified failure patterns of PCD inserts used in the test. Cutting edge fracture and flank face wear are the main failure patterns. Cutting edge fracture (Fig. 3a) is generated on the cutting tools of No. 2, 4, 5, 7, and 8 which are characterised by the bigger rake angle (Table 2), either RRA or ARA, because the big rake angle causes low strength of cutting edge. Meanwhile, flank face wear is the main pattern for the other tools, as shown in Fig. 3b. Based on the two tool failure patterns, PCD tool with the bigger rake angle is not suitable to mill TC11 under high feed rate.

For any cutting tool (including PCD tools), wear state is an ideal style. Based on the PCD tool failure patterns at different geometries, the cutting edge fracture can be avoided by setting suitable RRA and ARA. ISR value is, however, not directly related to cutting edge fracture.

Basically, The cutting conditions in face milling may be considered under two categories as follows: 1)

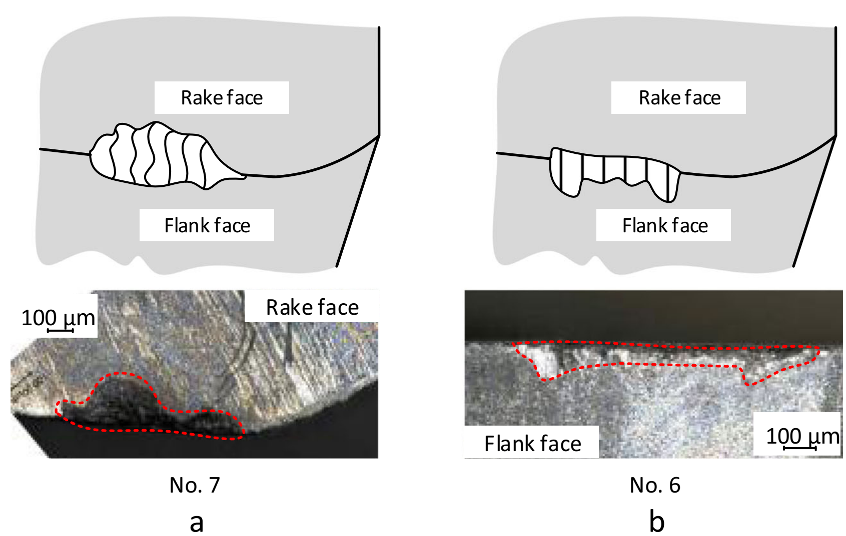

Fig. 3 PCD tool failure patterns in high feed milling of TC11. **a** Cutting edge fracture. **b** Flank face wear

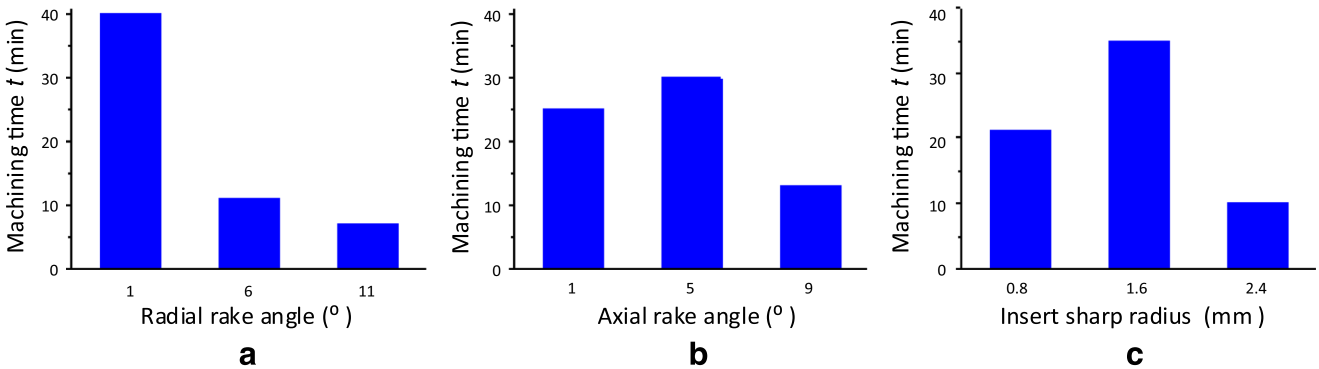

Fig. 4 Comparison of tool life with tool geometries. **a** Radial rake angle. **b** Axial rake angle. **c** Insert sharp radius

conditions as a result of which tool deterioration is due predominantly to wear and 2) conditions under which tool deterioration is due mainly to other phenomena such as edge fracture or plastic deformation [22, 23]. The two ISO standards (ISO 8688–1 and ISO 8688–2) are suitable to cemented carbide tools and high speed steel, although not applicable to all tool materials, e.g. PCBN, PCD. Moreover, there are no standards on tool life criterion for those tool materials. Considering the two conditions based on the ISO standards, in this paper, the tool life is therefore measured using machining time t based on two rules decided by the two tool failure patterns (Fig. 3); 1) cutting edge fracture rule: if there is fracture on the cutting edge, this tool is up to the life limitation, and 2) flank wear rule: if the flank wear value V_b is equal to or greater than 0.2 mm (due to high wear resistance), the cutting should be stopped. Figure 4 shows the relationship between tool life and tool geometry parameters. From Fig. 4a, a sudden decrease of machining time t is observed when the RRA increases, which can be explained by the fact that the possibility of insert fracture is high when RRA is more than 6°. Meanwhile, as Fig. 4b, c shows, with a PCD insert of 5° ARA and 1.6 mm ISR, the highest tool life can be achieved.

3.3 Cutting force

Cutting process is characterised by the extensive stress and plastic deformation. The high compressive and frictional contact stress on the tool face results in substantial cutting force. Figure 5 shows the comparison of cutting forces of three directions with insert geometries. From Fig. 5a, for both F_f and F_a cutting forces, the RRA played a key role, and both cutting forces increased first. However, they began to decrease when RRA was 6°. Meanwhile, an increasing trend of F_e cutting force is seen when RRA increases. In Fig. 5b, for both F_f and F_e cutting forces, minimum values are generated when ARA is 5°, while an increasing trend of F_a cutting force is observed when ARA increases. As Fig. 5c shows, when ISR increases, F_f cutting force decreases, and F_e cutting force reaches the maximum value when ISR is 1.6 mm. In addition, F_a exhibits the same trend as F_e.

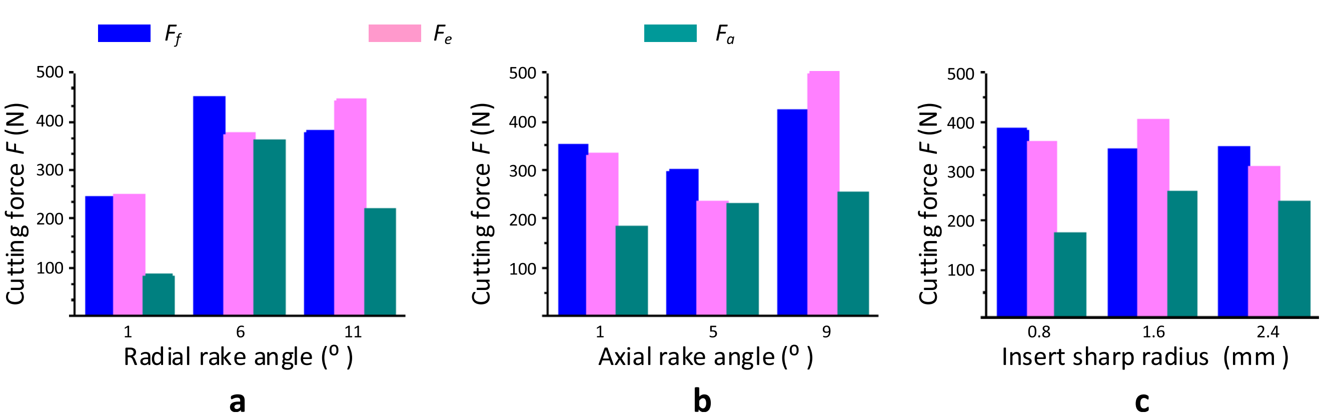

Fig. 5 Cutting forces at different insert geometries. **a** Radial rake angle. **b** Axial rake angle. **c** Insert sharp radius

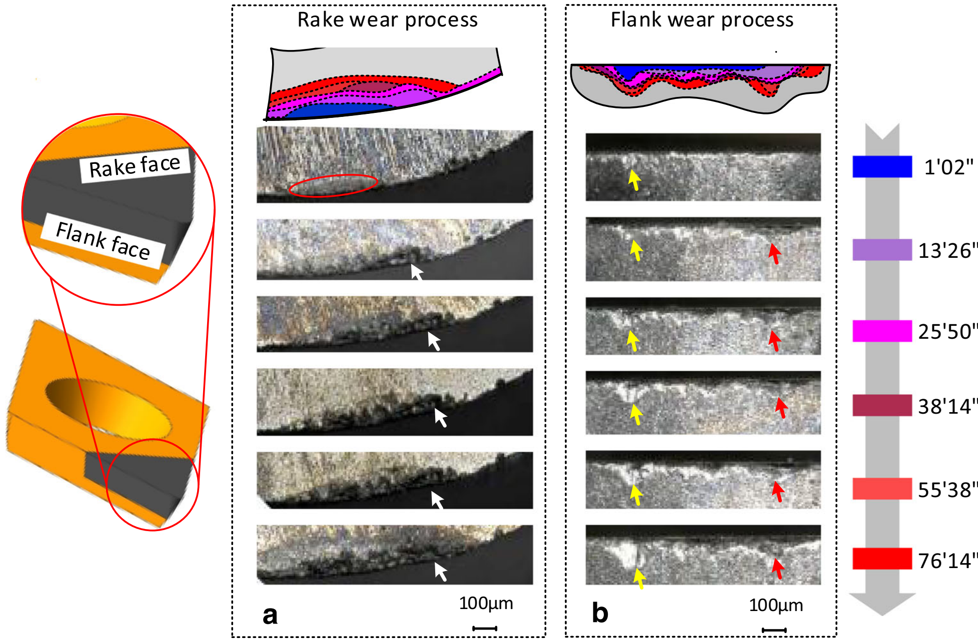

Fig. 6 Progress of rake and flank face wears. **a** Rake face wear. **b** Flank face wear

Comparing cutting force and tool life for RRA, when RRA is 1°, cutting forces are the lowest and the tool life is the highest (Fig. 4a). On the other hand, when cutting force reaches the value that may cause cutting edge fracture, the tool life is at risk. ARA shares the same trend with RRA. Therefore, a conclusion can be drawn that both too big and too small ISRs should be avoided. Nevertheless, there is no clear relationship between cutting force and tool life if comparing Fig. 4 with Fig. 5.

3.4 Wear progress

By comparing the results of tool wear patterns (Fig. 3) and the property of PCD material, flank wear pattern can be obtained for PCD tool design in milling TC11 at high feed rate. Figure 6 depicts the PCD tool wear progress with machining time *t*, on both the rake face and flank face. As shown in Fig. 6a, at the beginning, there was a wear zone on the rake face (in the red ellipse), and then a notch appeared at 13′ 26″. It was expanded over time around the initial zone. Figure 6b shows the wear progress of flank face, where the initial wear notch appeared at 1′02″ on the flank face. It was expanded further over time (see the area pointed by the yellow arrow). Along the process, another wear notch appeared at 13′ 26″, and it was also expanded over time (red arrow). According to the rake face wear progress, the notch is a potential area causing the fracture of the cutting edge, as well as the notches on the flank face.

4 Conclusions

The experimental observations and analyses reported in this paper show the capability of PCD tool in milling of TC11 at high feed rate. The following conclusions can be drawn based on the results of this study:

1) The surface roughness R_a is critically influenced by the radial rake angle, and its value is in the range from 0.8 to 1.6 μm, which indicates that the high feed milling method with PCD tool is suitable for finishing machining in some cases that do not require high surface roughness.
2) Cutting edge fracture and flank face wear are the main failure patterns, and the radial rake angle is a critical factor. Also, the flank wear is an ideal wear pattern, which can be obtained by setting suitable geometry parameters. In addition, based on the rules of tool failure, the longest tool life can be achieve by selecting suitable radial rake angle (around 1°), axial rake angle (around 5°), and insert sharp radius (around 1.6 mm).
3) On the rake face, area wear happens mainly at the beginning. Then, a notch appears with the wear expanded around the notch. Whereas on the flank face, a notch is usually developed first and expanded further. Other notches may appear and progress like the first one.

Acknowledgments This work was supported by National Science and Technology Major Project (2012ZX04003051).

References

1. Lutjering G, Williams J (2003) Titanium. Springer, Berlin
2. Godbole S (2013) The technological trendsetter. Trade magazine for efficient manufacturing, vol 9–10. Publish-Industry Verlag, Munich
3. Aspinwall DK, Dewes RC, Mantle AL (2005) The machining of γ-TiAI intermetallic alloys. CIRP Ann Manuf Technol 54(1):99–104. doi:10.1016/s0007-8506(07)60059-6
4. Bhaumik SK, Divakar C, Singh AK (1995) Machining Ti -6AI-4V alloy with a WBN-CBN composite tool. Mater Des 16(4):221–226
5. Che-Haron CH (2001) Tool life and surface integrity in turning titanium alloy. J Mater Process Technol 118:231–237
6. Pérez RGV (2005) Wear mechanisms of WC inserts in face milling of gamma titanium aluminides. Wear 259(7–12):1160–1167. doi:10.1016/j.wear.2005.02.062
7. Jaffery SHI, Mativenga PT (2011) Wear mechanisms analysis for turning Ti-6Al-4V—towards the development of suitable tool coatings. Int J Adv Manuf Technol 58(5–8):479–493. doi:10.1007/s00170-011-3427-y
8. Rao B, Dandekar CR, Shin YC (2011) An experimental and numerical study on the face milling of Ti–6Al–4V alloy: tool performance and surface integrity. J Mater Process Technol 211(2):294–304. doi:10.1016/j.jmatprotec.2010.10.002
9. Hou J, Zhou W, Duan H, Yang G, Xu H, Zhao N (2014) Influence of cutting speed on cutting force, flank temperature, and tool wear in end milling of Ti-6Al-4V alloy. Int J Adv Manuf Technol 70(9–12):1835–1845. doi:10.1007/s00170-013-5433-8
10. An QL, Fu YC, Xu JH (2011) Experimental study on turning of TC9 titanium alloy with cold water mist jet cooling. Int J Mach Tools Manuf 51(6):549–555. doi:10.1016/j.ijmachtools.2011.03.005
11. Li A, Zhao J, Wang D, Zhao J, Dong Y (2012) Failure mechanisms of a PCD tool in high-speed face milling of Ti–6Al–4V alloy. Int J Adv Manuf Technol 67(9–12):1959–1966. doi:10.1007/s00170-012-4622-1
12. Rotella G, Dillon OW, Umbrello D, Settineri L, Jawahir IS (2013) The effects of cooling conditions on surface integrity in machining of Ti6Al4V alloy. Int J Adv Manuf Technol 71(1–4):47–55. doi:10.1007/s00170-013-5477-9
13. Rotella G, Dillon OW Jr, Umbrello D, Settineri L, Jawahir IS (2014) The effects of cooling conditions on surface integrity in machining of Ti6Al4V alloy. Int J Adv Manuf Technol 71(1–4):47–55. doi:10.1007/s00170-013-5477-9
14. Nabhani F (2001) Machining of aerospace titanium alloys. Robot Comput Integr Manuf 17:99–106
15. Su H, Liu P, Fu Y, Xu J (2012) Tool life and surface integrity in high-speed milling of titanium alloy TA15 with PCD/PCBN tools. Chin J Aeronaut 25(5):784–790. doi:10.1016/s1000-9361(11)60445-7
16. Amin AKMN, Ismail AF, Nor Khairusshima MK (2007) Effectiveness of uncoated WC–Co and PCD inserts in end milling of titanium alloy—Ti–6Al–4V. J Mater Process Technol 192–193:147–158. doi:10.1016/j.jmatprotec.2007.04.095
17. Oosthuizen GA, Akdogan G, Treurnicht N (2010) The performance of PCD tools in high-speed milling of Ti6Al4V. Int J Adv Manuf Technol 52(9–12):929–935. doi:10.1007/s00170-010-2804-2
18. Corduan N, Himbart T, Poulachon G, Dessoly M, Lambertin M, Vigneau J, Payoux B (2003) Wear mechanisms of new tool materials for Ti-6AI-4V high performance machining. CIRP Ann Manuf Technol 52(1):73–76. doi:10.1016/s0007-8506(07)60534-4
19. Kuljanic E, Fioretti M, Beltrame L, Miani F (1998) Milling titanium compressor blades with PCD cutter. CIRP Ann Manuf Technol 47(1):61–64. doi:10.1016/s0007-8506(07)62785-1
20. Sutter G, List G (2013) Very high speed cutting of Ti–6Al–4V titanium alloy—change in morphology and mechanism of chip formation. Int J Mach Tools Manuf 66:37–43. doi:10.1016/j.ijmachtools.2012.11.004
21. Ren L (2009) Design and optimization of experiment. Science Press Ltd., Beijing
22. ISO (1989) Tool life testing in milling—part 1: face milling. ISO 8688–1:1989. International Organization for Standards, Geneva
23. ISO (1989) Tool life testing in milling—part 2: end milling. ISO 8688–2:1989. International Organization for Standards, Geneva